

Published in IET Systems Biology
Received on 11th January 2010
Revised on 26th May 2010
doi: 10.1049/iet-syb.2010.0013

Special issue on the Third *q-bio* Conference on Cellular Information Processing



Identification from stochastic cell-to-cell variation: a genetic switch case study

B. Munsky¹ M. Khammash²

¹Center for Nonlinear Studies and Computer, Computational and Statistical Sciences Division, Los Alamos National Laboratory, Los Alamos, NM 87545, USA

²Center for Control, Dynamical Systems and Computation and The Department of Mechanical Engineering, University of California, Santa Barbara, CA 93106, USA
E-mail: brian.munsky@gmail.com

Abstract: Owing to the inherently random and discrete nature of genes, RNAs and proteins within living cells, there can be a wide range of variability both over time in a single cell and from cell to cell in a population of genetically identical cells. Different mechanisms and reaction rates help shape this variability in different ways, and the resulting cell-to-cell variability can be quantitatively measured using techniques such as time-lapse microscopy and fluorescence activated cell sorting (or flow cytometry). It has been shown that these measurements can help to constrain the parameters and mechanisms of stochastic gene regulatory models. In this work, finite state projection approaches are used to explore the possibility of identifying the parameters of a specific stochastic model for the genetic toggle switch consisting of mutually inhibiting proteins: LacI and λ CI. This article explores the possibility of identifying the model parameters from different types of statistical information, such as mean expression levels, LacI protein distributions and LacI- λ CI multivariate distributions. It is determined that although the toggle model parameters cannot be uniquely identified from measurements that track just the LacI variability, the parameters could be identified from measurements of the cell-to-cell variability in both regulatory proteins. Based upon the simulated data and the computational investigations of this study, experiments are proposed that could enable this identification.

1 Introduction

A key issue facing modellers of gene regulatory systems is that rare chemical components (e.g. genes, RNA molecules and proteins) can lead to large amounts cellular variability [1–7]. This variability has attracted much recent attention, and it is well established that different system mechanisms will affect variability in different manners. In some systems, variability enhances dynamic signals via stochastic focussing [8]; in other cases, it may cause or enhance resonant fluctuations [9]; some other network topologies may result in stochastic switching [10–13]; and in many systems deleterious variability may be repressed [14].

There are a number of well-established experimental techniques in which fluorescent markers are used to highlight the molecular variability of single cells [15]. The most common of these techniques is flow cytometry [16],

which enables researchers to perform hundreds of millions of controlled single cell experiments all at the same time. For this technique, cell strains can be engineered to express fluorescent proteins such as green, yellow or cyan fluorescent protein (*gfp*, *yfp*, *cfp*), all of which can be measured in a fraction of a second for each cell. Different cultures of the same cell strain can be perturbed with different inputs, at different levels and at different times. A researcher can measure a million cells in a minute and test 40 or more different conditions in a single hour. And, unlike population level and/or in vitro techniques for measuring biological parameters (gels, immunoblotting etc.), the cells can be grown naturally throughout the experiment and measurements are made on individual living cells.

The more recently discovered technique of single molecule fluorescence in situ hybridisation (FISH) [17] allows

researchers to tag and count specific mRNA populations in individual fixed cells. With automated imaging techniques it is possible to count mRNA molecules in thousands of individual cells, thereby obtaining precise distributions under carefully controlled experimental conditions. Flow cytometry and FISH-based single cell microscopy are highly complementary approaches to study variability. Whereas cytometry with fluorescent proteins can measure post-translational activity, single cell microscopy with FISH mRNA markings can measure pre-translational regulation. Although flow cytometry allows for the measurement of more individual cells, single cell microscopy allows for more precise measurements of individual cells.

Using either or both experimental approaches, the measured variability in gene expression offers a surprisingly rich source of information about system parameters and dynamics. This vast amount of data is often far more complicated to analyse, and in many computational studies, cell-to-cell variability has been viewed as a computational nuisance – a viewpoint that is not helped by the term ‘noise’, which is frequently attached to this variability. If one does not include intrinsic variability in a model, then one cannot hope to capture certain cellular behaviours. However, in many cases, the inclusion of model stochasticity results in an explosion of computational complexity. For many other cases, the intrinsic variability of gene regulation can be analysed techniques such as kinetic Monte Carlo (KMC) algorithms [18] and stochastic differential equation approaches [19]. In turn, these KMC approaches have been improved with various sampling approaches [20, 21], τ leaping approaches [22] and time scale separation schemes [23, 24]. In a different direction, many researchers have sought to directly solve for the evolution of probability distributions using various techniques such as linear noise approximations [25, 26], moment closure [27, 28] and matching [29] techniques, moment generating functions [30], spectral methods [31] and finite state projection (FSP) approaches [32–35]. At present, none of these approaches suffices to handle all systems, and there remains much work to be done to improve our computational capabilities. However, as these tools develop, it becomes more possible to overcome the obstacle of intrinsic noise and gain significant benefits from analytical studies.

When it is possible to overcome the obstacles presented by cellular variability, the inclusion of system stochasticity can reveal a wealth of additional information regarding the dynamics of biochemical networks. Analyses of how variability is affected by different regulatory architectures provide a new tool with which to compare and contrast different possibilities for evolutionary design [36]. Alternatively, when this design is not known a priori, analyses of cellular variability may help to discover it [37–39]. For example, different logical structures such as AND or OR gates can be discovered in two component regulatory systems by examining the stationary transmission of the cell variability through the network [37], or correlations of different aspects of cell expression at many time points can reveal different

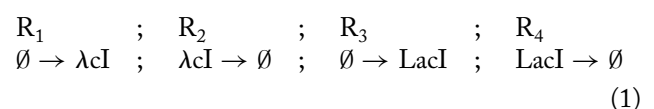
causal relationships between genes within a network [38]. Similarly, measuring and analysing the statistics of gene regulatory responses in certain conditions can help to identify system parameters and develop quantitative, predictive models for certain systems [40, 41].

In this article, we use computational analyses to demonstrate the usefulness of combining stochastic analyses and single cell measurements to identify gene regulatory models. We follow a similar approach to that in [42] in that we will apply FSP – [32, 34, 35] tools to conduct stochastic analyses and parameter identification for the genetic toggle switch from [42, 43]. In the following section, we provide a brief background on previous analyses of the toggle switch, and we discuss the application of FSP analysis tools to this system. Then, in Section 3 we use these tools and simulated data to determine the types of additional experiments that are necessary to fully identify the parameters of the toggle model. Finally, in Section 4 we summarise our findings and make a few concluding remarks.

2 Background

The toggle switch, composed of the mutually inhibiting genes *lacI* and λ CI, was first constructed and presented in [42] and then extended in [43] to be used as a sensor of environmental influences, such as radiation or external chemical signals. This switch is a construction of two genes, each of whose protein, λ CI or LacI, inhibits the production of the other (see Fig. 1a). With exposure to ultraviolet (UV) light or mitomycin C (MMC), damage to DNA initiates a global response, known as the SOS response, which up-regulates RecA coproteases and increases the degradation of λ CI. As a result, different amounts of UV or MMC change the trade-off between λ CI and LacI molecules. The output of the mechanism is GFP, which is also controlled by the same promoter as *lacI* and is assumed to be expressed at the same level as LacI. Depending upon environmental conditions, the system exhibits a bias towards one phenotype or another (i.e. it either has a high level of LacI and GFP and is highly fluorescent or it has a high level of λ CI and is not fluorescent). A vast number of models have been proposed to describe this and other toggle switches, including deterministic [43] and stochastic versions [13, 44, 45] to name a few. This study considers a particular stochastic model similar to that in [13] and aims to determine the types of experimental data necessary to determine the model parameters. To explore these requirements, we use simulated data of the type that can be measured using flow cytometry experiments such as those conducted in [43]

The stochastic model of the toggle switch is composed of four non-linear production/degradation reactions given by



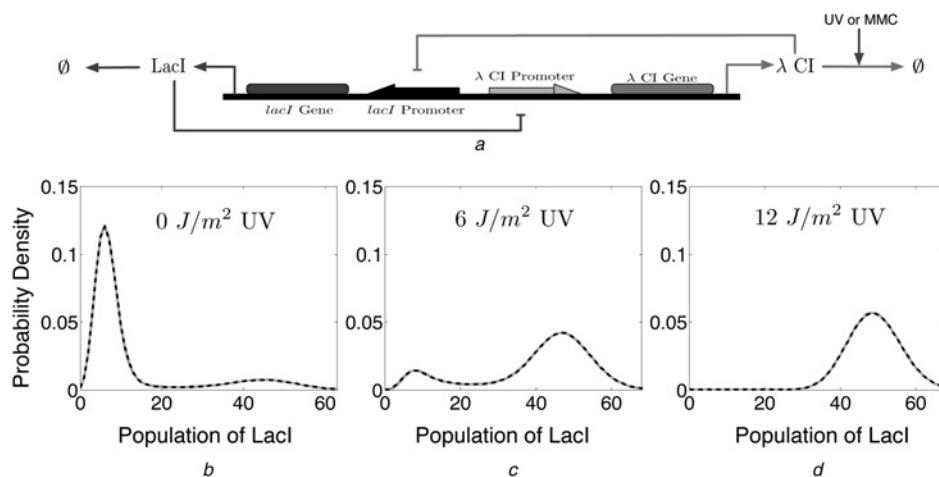


Figure 1 A stochastic model for the genetic toggle switch

a Basic schematic of the toggle model comprised of two inhibitors: λ CI inhibits the production of Lacl and vice versa. In the model, the synthesis rates of λ CI and Lacl are non-linear functions of their counterparts. Environmental influences (UV radiation) increase the degradation rate of λ CI and affect the tradeoff between the two regulators

b–d Marginal probability distributions of Lacl as simulated with parameters sets #0 and #3 from Table 1. The degradation parameter δ_u is the only parameter that changes between the panels B–D

The rates of these reactions, $w(\lambda$ CI, Lacl, $\mathbf{A}) = [w_1(\lambda$ CI, Lacl, $\mathbf{A}), \dots, w_4(\lambda$ CI, Lacl, $\mathbf{A})]$ depend upon the populations of the proteins, λ CI and Lacl, as well as the set of non-negative parameters, $\{k_{\lambda$ CI}^{(0,1)}, \alpha_{Lacl}, \eta_{Lacl}, k_{Lacl}^{(0,1)}, \alpha_{\lambdaCI}, η_{λ CI}, $\delta_{Lacl}, \delta_{\lambda$ CI}\}, according to

$$w_1 = k_{\lambda$$
CI}^{(0)} + \frac{k_{\lambdaCI}^{(1)}}{1 + \alpha_{Lacl} [Lacl]^{\eta_{Lacl}}}, \quad w_2 = \delta_{\lambdaCI} [\lambdaCI]
$$w_3 = k_{Lacl}^{(0)} + \frac{k_{Lacl}^{(1)}}{1 + \alpha_{\lambda$$
CI} [\lambdaCI]^{\eta_{\lambdaCI}}}, \quad w_4 = \delta_{Lacl} [Lacl]

In the model, the λ CI degradation parameter, δ_{λ CI}, takes on different values depending upon environmental influences such as UV radiation, whereas the remaining nine parameters are assumed to be independent of environmental conditions. Thus, the full parameters set is represented by

$$\mathbf{A} = \{k_{\lambda$$
CI}^{(0,1)}, \alpha_{Lacl}, \eta_{Lacl}, k_{Lacl}^{(0,1)}, \alpha_{\lambdaCI}, \eta_{\lambdaCI}, \delta_{Lacl}\},
$$\{\delta_{\lambda$$
CI}(0), \delta_{\lambdaCI}(6), \delta_{\lambdaCI}(12)\} \in \{\mathbb{R}_{\geq 0}^9, \mathbb{R}_{\geq 0}^3\}

At present there is insufficient evidence to define every parameter of the toggle switch model, and the current study relies upon simulated data in an effort to determine what additional experiments are necessary. To generate these data, we have chosen a reference parameter set as follows (see (2))

$$\begin{aligned} k_{\lambda$$
CI}^{(0)} &= 6.8 \times 10^{-5} \text{ s}^{-1}, & k_{\lambdaCI}^{(1)} &= 1.6 \times 10^{-2} \text{ s}^{-1}, & \alpha_{Lacl} &= 6.1 \times 10^{-3} N^{-\eta_{Lacl}} \\ k_{Lacl}^{(0)} &= 2.2 \times 10^{-3} \text{ s}^{-1}, & k_{Lacl}^{(1)} &= 1.7 \times 10^{-2} \text{ s}^{-1}, & \alpha_{\lambdaCI} &= 2.6 \times 10^{-3} N^{-\eta_{\lambdaCI}} \\ \eta_{Lacl} &= 2.1 & \eta_{\lambdaCI} &= 3.0 & \delta_{Lacl} &= 3.8 \times 10^{-4} N^{-1} \text{ s}^{-1} \\ \delta_{\lambdaCI}(0) &= 3.8 \times 10^{-4} N^{-1} \text{ s}^{-1}, & \delta_{\lambdaCI}(6) &= 6.7 \times 10^{-4} N^{-1} \text{ s}^{-1}, & \delta_{\lambdaCI}(12) &= 1.5 \times 10^{-3} N^{-1} \text{ s}^{-1} \end{aligned} \quad (2)

where the notation N corresponds to the integer number of molecules of the relevant reacting species. These parameters have been chosen partially to match values in the literature and partially to match the qualitative behaviours of the measured fluorescence histograms from [43] (i.e. the model expresses a small amount of Lacl at low UV levels, a large amount of Lacl at higher UV levels and has a bimodal distribution at intermediate UV levels – see Fig. 1). In the context of the current study, the most important of these parameters are the half-lives of Lacl and λ CI, which effectively set the timescale of the system's transient responses. Since both proteins are extremely stable and have half-lives that are much longer than the cell division time, δ_{λ CI(0) and $\delta_{Lacl}(0)$ have both been set to match a dilution half live of 30 min. (cell division time). The cooperativity of λ CI binding, η_{λ CI is chosen to be 3 to reflect the three binding sites of λ CI to the P_L promoter. The cooperativity of Lacl binding, η_{Lacl} is set to 2.1 as identified in [40]. The remaining parameters have been chosen to match the qualitative behaviour of the system as measured in [43] at the different levels of UV radiation.

At this point, no attempt has yet been made to fit the quantitative values of these parameters for the current model. For such a fit to provide much insight, one would first need to calibrate for background fluorescence and allow for the extrinsic variability in *gfp* fluorescence as explored in [40]. This would require far more experimental data than is currently available for this system. With the

use of 96- and 384-well plate auto-samplers, today's flow cytometry equipment is capable of providing this additional information for little additional experimental cost, and the acquisition of this data will not be a limiting step in the identification process.

2.1 Stochastic analysis of the toggle switch

By assuming that cells constitute a well-mixed environment, one can model biochemical populations with a jump-Markov process. As mentioned above, there are numerous approaches to analyse such processes, and many researchers are actively involved in developing new approaches. For the purpose of this examination, the choice of method does not matter, so long as it provides an accurate and efficient solution. Because the FSP [32–35, 46] approach provides a direct accuracy guarantee on the solution of the master equation, it is a natural choice with which to conduct this investigation. In this subsection, we provide a brief background on the use of the FSP approach for the modelling of the toggle switch.

Under the reactions presented in the preceding section, the joint probability density of having i molecules of LacI and j molecules of λ CI evolves according the set of linear ordinary differential equations

$$\begin{aligned} \frac{dp_{i,j}(t, \mathbf{A})}{dt} = & - \sum_{k=1}^4 w_k(i, j, \mathbf{A}) p_{i,j}(t, \mathbf{A}) + w_1(j, \mathbf{A}) p_{i-1,j}(t, \mathbf{A}) \\ & + w_2(i+1, \mathbf{A}) p_{i+1,j}(t, \mathbf{A}) + w_3(i, \mathbf{A}) p_{i,j-1}(t, \mathbf{A}) \\ & + w_4(j+1, \mathbf{A}) p_{i,j+1}(t, \mathbf{A}) \end{aligned}$$

which is typically known as the (chemical) Master Equation [25]. Because the toggle reaction rates, w_1 and w_2 , are non-linear, the master equation has no known closed-form solution, but the FSP approach [32, 34] allows us to approximate the solution to any pre-specified degree of accuracy. Given the infinitesimal generator matrix, $\mathbf{A}(\mathbf{A})$, the initial probability distribution, $\mathbf{P}(0)$, and a chosen error tolerance, $\varepsilon > 0$, we can systematically find a finite projection system

$$\dot{\mathbf{P}}^{FSP}(t, \mathbf{A}) = \mathbf{A}_J(\mathbf{A}) \cdot \mathbf{P}^{FSP}(t, \mathbf{A})$$

such that

$$\left\| \begin{bmatrix} \mathbf{P}_J(t, \mathbf{A}) \\ \mathbf{P}_{J^c}(t, \mathbf{A}) \end{bmatrix} - \begin{bmatrix} \mathbf{P}^{FSP}(t, \mathbf{A}) \\ \mathbf{0} \end{bmatrix} \right\|_1 \leq \varepsilon, \quad \text{and} \quad \mathbf{P}^{FSP}(0) = \mathbf{P}_J(0) \quad (3)$$

where the index vector \mathbf{J} denotes the set of states included in the projection, \mathbf{P}_J is the corresponding probabilities of those states, and \mathbf{A}_J is the corresponding principle submatrix of \mathbf{A} [32, 34].

For this study, we have chosen the projection set, \mathbf{J} , to include all states that satisfy: $i \leq N_1$, $j \leq N_2$ and $(i-3)(j-3)^2 \leq N_3$, where the values of N_1 , N_2 and N_3 are allowed to increase until the projection error, ε , is less than 10^{-6} . The actual expansion is carried out as described in [46], where the values of N_1 , N_2 and N_3 are increased depending upon the dominant directions of probability leakage out of the current projection space (see Section 2.1 of [46] for more details). For the reference parameter set the final projection space is defined by the triplet $(N_1, N_2, N_3) = (90, 90, 18, 400)$ for the case with 0 J/m^2 UV radiation, $(N_1, N_2, N_3) = (50, 110, 17, 600)$ for the case with 6 J/m^2 UV radiation and $(N_1, N_2, N_3) = (30, 110, 12, 800)$ for the case with 12 J/m^2 UV radiation. Other parameter sets require different projection spaces to reach the desired error tolerance, and the projection space is expanded and contracted during each parameter search.

2.2 Fitting the toggle model to simulated data

In most cases, the full joint probability distribution is not measured, and only an expected value or marginal distribution is to be considered. To explore how different quantities of information may lead to different identification results, we consider identification strategies using five such statistical quantities:

1. only the mean level of LacI, denoted as μ_{LacI} ,
2. the mean levels of LacI and λ CI, denoted as $\mu_{\{\text{LacI}, \lambda\text{CI}\}} := \{\mu_{\text{LacI}}, \mu_{\lambda\text{CI}}\}$,
3. the marginal distribution of LacI, denoted as f_{LacI} ,
4. the marginal distributions of LacI and λ CI, denoted as $f_{\{\text{LacI}, \lambda\text{CI}\}} := \{f_{\text{LacI}}, f_{\lambda\text{CI}}\}$ and
5. the full joint distributions of LacI and λ CI, denoted as full \mathbf{P} .

Each of these is naturally represented as a linear projection of the full distribution. For example, the mean level of LacI and the marginal distribution of LacI are given by

$$\mu_{\text{LacI}}(\mathbf{A}, t) = \sum_{i=0}^{\infty} \sum_{j=0}^{\infty} i p_{i,j}(\mathbf{A}, t) \quad \text{and}$$

$$f_{\text{LacI}}(\mathbf{A}, t) = \sum_{j=0}^{\infty} p_{i,j}(\mathbf{A}, t)$$

Equivalently, one could write each of the statistical quantities (1)–(5) above in matrix form as $\mathbf{y}(\mathbf{A}, t) = \mathbf{C}\mathbf{P}(\mathbf{A}, t)$, where the output matrix \mathbf{C} depends upon the statistical quantity to be considered. We note that if all of the reaction rates were affine linear, then the mean behaviours of μ_{LacI} and $\mu_{\lambda\text{CI}}$ would be equivalent to the deterministic mass action

kinetics model of the same system. Because the toggle model has non-linear production terms, this equivalence does not hold. It is also important to note that the toggle switch gives rise to a relatively complicated bimodal distribution, which is not adequately be described with a small number of statistical moments, so low order moment based approaches such as those in [25–29] should be expected to yield incorrect results for this model.

With the FSP solution approach in hand, the identification procedure is relatively simple – we find the parameter arguments, \mathbf{A}^* , that minimises the difference between the measured statistical quantity, $\tilde{\mathbf{y}}(t)$, and the numerical solution of that quantity, $\mathbf{y}(\mathbf{A}, t)$

$$\mathbf{A}^* := \arg \min_{\mathbf{A}} |\tilde{\mathbf{y}}(t) - \mathbf{y}(t, \mathbf{A})|_p \quad (4)$$

More specifically, because we will frequently be comparing probability distributions, we use the one-norm (i.e. $p = 1$) difference for a number of reasons: First, the FSP approach (3) directly computes the exact one-norm error in the solution of the master equation, which then provides exact bounds on the one-norm difference between a measured and predicted distributions. Second, the one-norm of any probability distribution is exactly one and the one-norm difference between two distributions lies between zero for a perfect match and two for a perfect mismatch. Finally, in our experience one-norm optimisations provide distributions that better match the full qualitative shape of measured distributions, whereas other norms (such as the Euclidian norm) apply too much importance to peaks of these distributions, independent of how much probability measure is contained in those peaks.

In this study, we begin each minimisation in (4) with the same initial guess (see equation at the bottom of the page)

and then update this guess with iterations of gradient-based and simulated annealing searches until the objective function has decreased by at least two orders of magnitude. In the numerical studies presented here, it is known a priori that the ‘true’ parameter set gives an exact match and satisfies this criteria for any p -norm. If the optimisation terminates at a much different parameter set, then the identification is not unique for the data set $\tilde{\mathbf{y}}$. In more realistic practice, local minima must be discarded by using multiple, randomly generated initial parameter guesses. In that case, an optimal parameter set would be considered to be unique if the given solution yields the smallest achieved value for the objective function and if that parameter has

been repeatedly found during independent optimisation procedures.

3 Results

The model in the previous section and the parameters in (2) have been used to numerically generate the joint probability distribution of the numbers of LacI and λ Cl molecules. We have assumed an initial condition of zero molecules of each species, and have solved the master equation for the distribution at times of {1, 2, 3, 4, 5} hours later. In this section, we consider each of the five identification strategies listed above and examine how successful each approach may be for this identification. For each strategy, we first consider the identification using the relevant data at 5 h only and later with the same information at all five time points. Each identification strategy results in a parameter set that captures the relevant data to within a one-norm difference of 10^{-1} , and Tables 1 and 2 list the relative values of these identified parameters. In most cases, the identification is insufficiently constrained, and the identified parameter set is not unique (i.e. it is different than the original parameter set). For these, the parameter set may match some portions of the simulated data, but not others. Table 3 tabulates these differences for the ten different parameter sets. We note that the numbers in Tables 1–3 should be viewed as qualitative results as the identified parameters sets {1–4, 6, 7} depend upon the initial guess and are not unique.

3.1 Identification from a single time point

Table 1 lists the relative values of the identified parameters compared to their actual values (reference set #0). These parameters have been identified from different statistical quantities taken from the simulated data at a time of 1 h. The following subsections discuss the corresponding success or failures in these identification attempts.

3.1.1 Identification using mean level of LacI at $t = 5$ h:

In many modelling endeavours, researchers concentrate their efforts solely on matching the mean behaviours of the observable systems. In other situations, there are often good reasons for this choice. First, most experimental measurements are taken at the population level using lysed cells, and data on the cell-to-cell variability is not available. Second, if one is only interested in the mean level behaviour, then it is often possible to utilise deterministic models, which are typically more computationally tractable. These reasons are far less compelling in this situation. When all measurements are taken using flow cytometry or another

$$\begin{array}{lll} \hat{k}_{\lambda\text{Cl}}^{(0)} = 10^{-4} \text{ s}^{-1}, & \hat{k}_{\lambda\text{Cl}}^{(1)} = 10^{-2} \text{ s}^{-1}, & \alpha_{\text{LacI}} = 10^{-2} \text{ N}^{-\eta_{\text{LacI}}} \\ \hat{k}_{\text{LacI}}^{(0)} = 10^{-3} \text{ s}^{-1}, & \hat{k}_{\text{LacI}}^{(1)} = 10^{-2} \text{ s}^{-1}, & \alpha_{\lambda\text{Cl}} = 10^{-3} \text{ N}^{-\eta_{\lambda\text{Cl}}} \\ \eta_{\text{LacI}} = 3, & \eta_{\lambda\text{Cl}} = 3, & \delta_{\text{LacI}} = 10^{-4} \text{ N}^{-1} \text{ s}^{-1} \\ \delta_{\lambda\text{Cl}}(0) = 10^{-4} \text{ N}^{-1} \text{ s}^{-1} & \delta_{\lambda\text{Cl}}(6) = 10^{-3} \text{ N}^{-1} \text{ s}^{-1} & \delta_{\lambda\text{Cl}}(12) = 10^{-3} \text{ N}^{-1} \text{ s}^{-1} \end{array}$$

Table 1 Parameter sets for the stochastic toggle model, which have been identified from different data sets at a fixed time of 5 h

Parameter	Units	Set 0: Ref. Set	Relative parameter values				
			set 1: μ_{LacI}	set 2: $\mu_{\{\text{LacI}, \text{Acl}\}}$	set 3: f_{LacI}	Set 4: $f_{\{\text{LacI}, \text{Acl}\}}$	Set 5: full P
$k_{\lambda\text{cl}}^{(0)}$	s^{-1}	6.8×10^{-5}	3.1	5.3	8.9	3.2	1.0
$k_{\lambda\text{cl}}^{(1)}$	s^{-1}	1.6×10^{-2}	6.3×10^{-1}	7.6×10^{-1}	5.0×10^{-1}	9.1×10^{-1}	1.0
$k_{\text{LacI}}^{(0)}$	s^{-1}	2.2×10^{-3}	3.0×10^{-1}	9.0×10^{-1}	5.6×10^{-1}	8.0×10^{-1}	1.0
$k_{\text{LacI}}^{(1)}$	s^{-1}	1.7×10^{-2}	2.8×10^{-1}	6.5×10^{-1}	5.7×10^{-1}	8.0×10^{-1}	1.0
δ_{LacI}	$\text{N}^{-1}\text{s}^{-1}$	3.8×10^{-4}	2.2×10^{-1}	6.7×10^{-1}	5.6×10^{-1}	8.0×10^{-1}	1.0
$\delta_{\lambda\text{cl}}(0)$	$\text{N}^{-1}\text{s}^{-1}$	3.8×10^{-4}	2.9×10^{-1}	6.1×10^{-1}	6.7×10^{-1}	9.5×10^{-1}	1.0
$\delta_{\lambda\text{cl}}(6)$	$\text{N}^{-1}\text{s}^{-1}$	6.7×10^{-4}	5.9×10^{-1}	7.2×10^{-1}	7.2×10^{-1}	9.7×10^{-1}	1.0
$\delta_{\lambda\text{cl}}(6)$	$\text{N}^{-1}\text{s}^{-1}$	1.5×10^{-3}	1.0	1.2	5.9×10^{-1}	9.5×10^{-1}	1.0
α_{LacI}	$\text{N}^{-\eta_{\text{LacI}}}$	6.1×10^{-3}	1.2	2.1	7.1×10^{-2}	5.9×10^{-1}	1.0
$\alpha_{\lambda\text{cl}}$	$\text{N}^{-\eta_{\lambda\text{cl}}}$	2.6×10^{-3}	1.9×10^{-1}	5.4×10^{-1}	4.0×10^{-3}	4.8×10^{-1}	1.0
η_{LacI}	–	2.1	1.2	9.0×10^{-1}	1.3	1.1	1.0
$\eta_{\lambda\text{cl}}$	–	3.0	1.1	1.1	1.7	1.1	1.0

For parameter sets 1–5, the table lists the relative parameter values. The five different data sets correspond to (1) the mean level of LacI, (2) the mean levels of LacI and λcl , (3) the marginal distribution of LacI, (4) the marginal distributions of LacI and λcl , and (5) the full joint distribution of LacI and λcl . The model responses for each of these parameter sets are shown in Figs. 2–5

Table 2 Parameter sets for the stochastic toggle model, which have been identified from different data sets at all of five different measurement times: {1, 2, 3, 4, 5} h

Parameter	Units	Set 0: Ref. Set	Relative parameter values				
			Set 6: μ_{LacI}	Set 7: $\mu_{\{\text{LacI}, \lambda\text{cl}\}}$	Set 8: f_{LacI}	Set 9: $f_{\{\text{LacI}, \lambda\text{cl}\}}$	Set 10: full P
$k_{\lambda\text{cl}}^{(0)}$	s^{-1}	6.8×10^{-5}	7.7×10^{-7}	1.0	9.9×10^{-1}	1.0	1.0
$k_{\lambda\text{cl}}^{(1)}$	s^{-1}	1.6×10^{-2}	1.3	9.7×10^{-1}	1.0	1.0	1.0
$k_{\text{LacI}}^{(0)}$	s^{-1}	2.2×10^{-3}	1.5	1.1	1.0	1.0	1.0
$k_{\text{LacI}}^{(1)}$	s^{-1}	1.7×10^{-2}	9.6×10^{-1}	9.6×10^{-1}	1.0	1.0	1.0
δ_{LacI}	$\text{N}^{-1}\text{s}^{-1}$	3.8×10^{-4}	1.0	9.8×10^{-1}	1.0	1.0	1.0
$\delta_{\lambda\text{cl}}(0)$	$\text{N}^{-1}\text{s}^{-1}$	3.8×10^{-4}	5.1×10^{-1}	9.7×10^{-1}	1.0	1.0	1.0
$\delta_{\lambda\text{cl}}(6)$	$\text{N}^{-1}\text{s}^{-1}$	6.7×10^{-4}	7.5×10^{-1}	9.9×10^{-1}	1.0	1.0	1.0
$\delta_{\lambda\text{cl}}(12)$	$\text{N}^{-1}\text{s}^{-1}$	1.5×10^{-3}	8.3×10^{-1}	1.0	1.0	1.0	1.0
α_{LacI}	$\text{N}^{-\eta_{\text{LacI}}}$	6.1×10^{-3}	5.7×10^{-1}	9.2×10^{-1}	1.0	1.0	1.0
$\alpha_{\lambda\text{cl}}$	$\text{N}^{-\eta_{\lambda\text{cl}}}$	2.6×10^{-3}	5.2×10^{-1}	5.7×10^{-1}	1.0	1.0	1.0
η_{LacI}	–	2.1	1.2	1.0	1.0	1.0	1.0
$\eta_{\lambda\text{cl}}$	–	3.0	1.0	1.1	1.0	1.0	1.0

Five different data sets are as listed in Table 1. For parameter sets 6–10, the table lists the relative parameter values

Table 3 Goodness of fit for each parameter set and each subset of considered data

Parameter set #	One time point at 5 h					All time points at {1, 2, 3, 4, 5}h				
	μ_{LacI}	$\mu_{\{LacI,\lambda cI\}}$	f_{LacI}	$f_{\{LacI,\lambda cI\}}$	full P	μ_{LacI}	$\mu_{\{LacI,\lambda cI\}}$	f_{LacI}	$f_{\{LacI,\lambda cI\}}$	full P
1	$<10^{-3}$	1.42	0.78	2.4	2.2	3.2	8.1	10	16	15
2	$<10^{-3}$	$<10^{-3}$	0.91	1.8	1.3	0.59	1.1	5.5	9.4	6.7
3	0.004	1.4	0.015	1.3	1.4	0.81	8.8	3.9	11.4	8.5
4	0.007	0.017	0.024	0.043	0.072	0.61	1.3	1.4	2.1	1.6
5	$<10^{-3}$	$<10^{-3}$	$<10^{-3}$	$<10^{-3}$	$<10^{-3}$	0.002	0.006	0.007	0.012	0.010
6	0.002	1.7	0.68	2.7	2.3	0.023	7.6	2.8	11.2	11.2
7	0.001	0.006	0.18	0.28	0.19	0.011	0.046	0.72	1.1	0.78
8	$<10^{-3}$	0.001	$<10^{-3}$	0.001	0.001	$<10^{-3}$	0.005	$<10^{-3}$	0.005	0.008
9	$<10^{-3}$	$<10^{-3}$	$<10^{-3}$	$<10^{-3}$	$<10^{-3}$	$<10^{-3}$	$<10^{-3}$	$<10^{-3}$	$<10^{-3}$	$<10^{-3}$
10	$<10^{-3}$	$<10^{-3}$	$<10^{-3}$	$<10^{-3}$	$<10^{-3}$	$<10^{-3}$	$<10^{-3}$	$<10^{-3}$	$<10^{-3}$	$<10^{-3}$

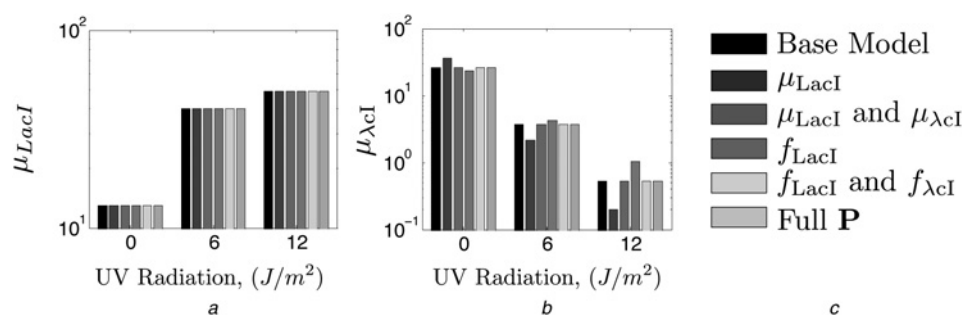
Parameter sets correspond to the ten different fits found by using different amounts of the simulated data (see Tables 1 and 2). The different columns show how well each parameter set fits different aspects of the simulated data – the metric used is the one norm difference between the model with the true parameter set and the identified parameter set. For the mean values, the metric refers to relative difference (i.e. $d = |\mu_{\text{model}} - \mu_{\text{data}}|/\mu_{\text{data}}$)

single cell technique, data on cell-to-cell variability is readily available. It would be a waste to ignore this information. Furthermore, because of strong non-linearities in the LacI and λcI production rates, the corresponding deterministic model fails to capture the mean behaviour of the true stochastic system (results not shown).

We first explore if it is possible to identify the unknown parameters from the mean LacI level, μ_{LacI} , at all three UV radiations levels and at a time of 5 h. Although it is not difficult to find a set of 12 parameters that match the mean level of LacI under the different levels of UV radiation, these parameters are not unique. Indeed, we find that parameter set #1 in Table 1 matches the mean LacI expression levels as can be seen in Fig. 2a. However, the same parameter set gives a very poor prediction for the

mean level of λcI as shown in Fig. 2b and Table 3. Thus, it is clear that the mean level of lacI is insufficient to identify the model parameters.

3.1.2 Identification using mean levels of LacI and λcI at $t = 5$ h: We next consider the possibility of identifying all 12 parameters from the mean level of both LacI and λcI for all three UV levels and at a time of five hours after induction. Once again it is easy to find that parameter set #2 in Table 1 matches these mean levels for both species, as can be seen in Figs. 2a and b. On the other hand, closer inspection of the marginal probability distributions of LacI and λcI reveals that this parameter set provides a poor prediction for the marginal distributions of the two chemical species, especially at low levels of UV induction (see Figs. 3a, b, d and e and Table 3).

**Figure 2** Mean levels for the toggle model

a Mean levels of LacI at 5 hours after induction with 0, 6 and 12 J/m² ultraviolet radiation

b Mean levels of λcI at 5 hours after induction with 0, 6 and 12 J/m² ultraviolet radiation

c Legend: five different parameter sets have been used, where each set captures a different portion of the system response as listed in Table 1

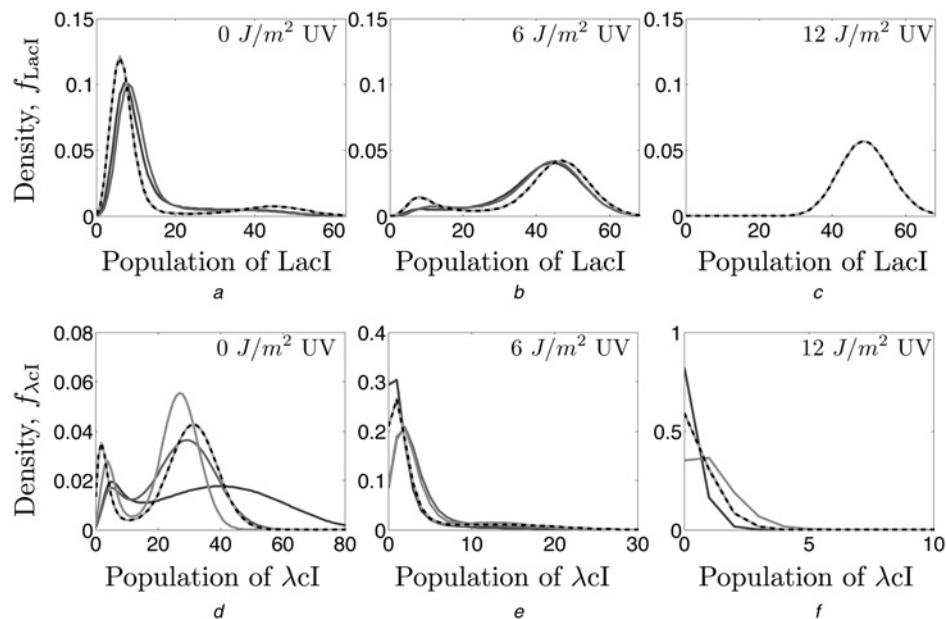


Figure 3 Marginal probability densities for the toggle model for five different parameter sets as listed in Table 1 (see Fig. 2c for legend)

a–c LacI distributions at 5 h after induction with 0, 6 and 12 J/m² UV radiation
d–f λcI distributions at 5 h after induction with 0, 6 and 12 J/m² UV radiation

3.1.3 Identification using marginal distribution of LacI at $t = 5$ h: As discussed in [40], if one utilises information of the cell-to-cell variability, then it becomes possible to better distinguish between models and parameter sets. With this in mind, we have attempted to conduct the identification from the marginal distribution of LacI at 5 h after induction with the different levels of UV radiation. Parameter set #3 in Table 1 has been found to match this marginal distribution. However, we once again discover that the identification is not unique, which suggests that data regarding the variability of a single protein (i.e. the kind of data taken in [43]) is not sufficiently rich for complete identifiability. On the other hand, closer inspection of Table 2 reveals a fixed ratio of about 0.6 between many of the parameters from set #3 and the true parameter set. This suggests that the identification has drastically narrowed the space of possible parameter sets, but more information is needed to provide a unique parameter set for the proposed model. For example, we see that parameter set #3 gives poor prediction for the mean and marginal distribution for λcI as can be seen in Fig. 2b and Figs. 3d–f and Table 3. Thus, any additional measurements of λcI would help to further constrain the model.

3.1.4 Identification using marginal distribution of both LacI and λcI at $t = 5$ h: Parameter set #4 has been identified from the simulated data using the marginal distributions of both species at all UV radiation levels and at the time of five hours after induction. Now the identified set correctly matches the mean and marginal distributions of LacI and λcI as shown in Figs. 2 and 3. However, there still remains a slight discrepancy between the full joint

distribution as computed with the reference parameter set and the same joint distribution as computed with parameter set #4 (see Table 3).

3.1.5 Identification using the full joint LacI/λcI distribution at $t = 5$ h: Table 3 shows that the joint distribution predicted by parameter sets #1–4 are different than the joint distribution found with the reference parameter set, suggesting that use of this full distribution would go a long way to further constraining the model. In our final attempt to identify the full parameter set from a single time point, we have conducted the identification based upon the full joint distribution of LacI and λcI at the time of 5 h. In this case, it appears that identification of the parameters is indeed possible, and all of the parameters are identified within a very small distance of their actual values. As an aside, it is interesting to note that the optimisation problem that uses the full distribution is much more easily solved than that which utilised only the marginal distributions. In these studies the identification based upon the whole distribution took less than an hour and converged to a much lower value than that based upon marginal distributions, which took several days. A full exploration of how these different data sets lead to better conditioning of the optimisation procedure is left for future work.

3.2 Identification from multiple time points

From above and from [40], it is clear that more statistical information provides a better chance for a system's identifiability. Similarly, it is equally important to conduct that identification using different time points, preferably

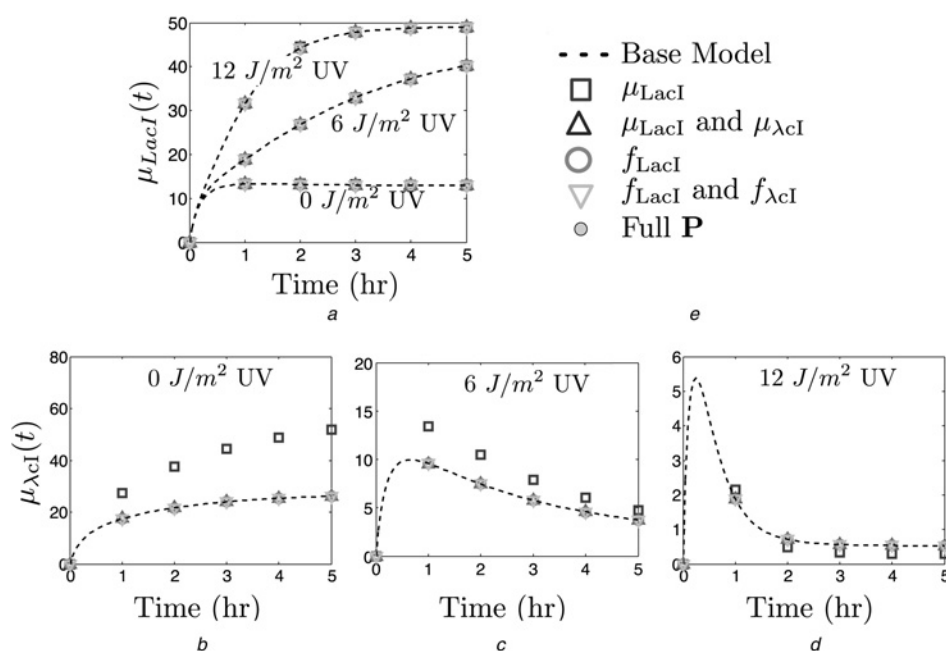


Figure 4 Mean level dynamics for the toggle model for five different parameter sets

a Mean level of LacI versus time after induction with 0, 6 and 12 J/m² UV radiation

b–d Mean level of λcI versus time after induction with 0, 6 and 12 J/m² UV radiation

e Legend: five different parameter sets have been used, where each set captures a different portion of the system response as listed in Table 2

during the system's transient response [40]. In the preceding subsection, we have attempted the identification based upon a single time point that occurred 5 h after induction. We note that the degradation rates of LacI and λcI in the absence of UV radiation correspond to a half life of 30 min (i.e. the cell division time) and even faster with UV radiation. Thus, since the identification is being conducted after ten such half lives, we are likely missing much of the system's transient dynamics. We have therefore redone the identification using measurements at each hour after induction.

Table 2 lists the relative values of the identified parameters as found using this more detailed information. For a comparison of the system dynamics with the different parameter values, Fig. 4 shows the responses of the mean LacI and λcI levels. From the figure, it is clear that parameter set #6 matches the response of LacI over time (panel A), but not that of λcI (squares in panels D–F). Furthermore, Fig. 4 and Table 3 show that parameter set #7 matches the mean dynamics of both proteins, but is insufficient to complete the identification. On the other hand, we note that with the additional time points, the marginal distribution of LacI (parameter set #8) does a much better job of obtaining the correct parameter values for the parameters. Finally, even when the full distribution is used to identify the parameters, the use of multiple time points considerably improves the approach – yielding more precise results and making the identification much less sensitive to unbiased measurement errors.

4 Conclusions

Many gene regulatory systems are characterised by small numbers of regulatory molecules, and therefore result in a large amount of variability both over time for single cells and from cell to cell in a clonal population. This variability is measurable with a number of experimental approaches, including time lapse fluorescence microscopy which can record the fluctuations of individual living cells and flow cytometry which allows for the rapid measurement of large populations of individual cells. To fully access the information available from these measurement techniques, it is necessary to utilise quantitative stochastic models which can capture these behaviours. FSP [32] type solutions are ideal for these types of analyses because they specifically compute the transient dynamics of cell-to-cell probability distributions – precisely the types of information measurable with flow cytometry. By combining flow cytometry measurements with FSP approaches, it becomes easier to constrain gene regulatory models and even completely identify models and parameters for natural and synthetic circuits [40].

Similarly, computational analyses of stochastic gene regulatory models can help researchers to determine the types of experiments necessary to provide better understanding of a given system. In this work, we have used FSP-based computational studies to explore the possibility of identifying parameters for a particular model of the genetic toggle switch [42, 43]. Our numerical studies have revealed that different identification strategies will produce varying degrees of

success. As summarised in Table 3, each successive addition of more statistical information can help to further constrain the space of allowable parameters – eventually leading to a single unique point for this model. For example, parameters can be found to match the mean (or marginal distribution) of one protein but not the other. Similarly, models can be found that match the mean behaviours of the system, but which do not match the marginal distributions of one or more species. Finally, models can be found to match the marginal distributions of both species, but which do not match the full joint distribution of both species. However, for this particular model, only one set of parameters is capable of matching the full joint distribution at the time of 5 h. Similarly, if one uses more experimental time points, then this also can further constrain the model and lead one to arrive at better models and more useful sets of parameters. In particular, we predict that if one could measure both LacI and λ CII populations in large numbers of individual cells at a time resolution of about an hour, then one could in principle fully identify the parameters for the proposed model of the gene toggle switch. We note that models of greater complexity such as those including additional parameters related to transcription, translation, oligomerization and other kinetics will require more measurements for complete identification.

The necessary experimental measurements for the identification of the current model could be obtained by reengineering the toggle switch to express two different fluorescent proteins: one controlled by the same promoter as LacI and the other controlled by the same promoter as λ CII. With an auto-sampler and multiple frequency fluorescence detectors, these new constructs can then be automatically measured with a time resolution of less than 10 min – even including many samples from independent colonies. Furthermore, background fluorescence levels can be calibrated out of the data using mutants lacking one or both of the reporter proteins, and extrinsic noise can be decreased using forward and side scatter information (or even flow cytometry images) to restrict measurements to cells with similar shapes, sizes and densities. In turn, such a carefully constrained and identified quantitative model could be used to predict switching behaviour under different environmental conditions as well as help direct the modification of the circuit to meet other synthetic design objectives.

5 References

- [1] MCADAMS M., ARKIN A.: 'Its a noisy business!', *Trends Gen.*, 1999, **15**, (2), pp. 65–69
- [2] ELOWITZ M., LEVINE A., SIGGIA E., SWAIN P.: 'Stochastic gene expression in a single cell', *Science*, 2002, **297**, pp. 1183–1186
- [3] THATTAI M., VAN OUDENAARDEN A.: 'Intrinsic noise in gene regulatory networks', *Proc. Natl. Acad. Sci.*, 2001, **98**, pp. 8614–8619
- [4] HASTY J., PRADINES J., DOLNIK M., COLLINS J.: 'Noise-based switches and amplifiers for gene expression', *Proc. Natl. Acad. Sci.*, 2000, **97**, pp. 2075–2080
- [5] OZBUDAK E., THATTAI M., KURTSEY I., GROSSMAN A., VAN OUDENAARDEN A.: 'Regulation of noise in the expression of a single gene', *Nat. Genet.*, 2002, **31**, pp. 69–73
- [6] FEDEROFF N., FONTANA W.: 'Small numbers of big molecules', *Science*, 2002, **297**, (5584), pp. 1129–1131
- [7] KEPLER T., ELSTON T.: 'Stochasticity in transcriptional regulation: origins, consequences, and mathematical representations', *Biophys. J.*, 2001, **81**, pp. 3116–3136
- [8] PAULSSON J., BERG O., EHRENBERG M.: 'Stochastic focusing: fluctuation-enhanced sensitivity of intracellular regulation', *Proc. Natl. Acad. Sci.*, 2000, **97**, (13), pp. 7148–7153
- [9] LI H., HOU Z., XIN H.: 'Internal noise stochastic resonance for intracellular calcium oscillations in a cell system', *Phys. Rev. E*, 2005, **71**, article id 061916
- [10] ARKIN A., ROSS J., MCADAMS H.: 'Stochastic kinetic analysis of developmental pathway bifurcation in phage λ -infected escherichia coli cells', *Genetics*, 1998, **149**, pp. 1633–1648
- [11] WOLF D., ARKIN A.: 'Fifteen minutes of flim: control of type 1 pili expression in e. coli', *OMICS: A J. Integr. Biol.*, 2002, **6**, pp. 91–114
- [12] MUNSKY B., HERNDAY A., LOW D., KHAMMASH M.: 'Stochastic modeling of the pap-pili epigenetic switch'. *Proc. FOSBE*, August 2005, pp. 145–148
- [13] TIAN T., BURRAGE K.: 'Stochastic models for regulatory networks of the genetic toggle switch', *Proc. Natl. Acad. Sci.*, 2006, **103**, pp. 8372–8377
- [14] DUBLANCHE Y., MICHALODIMITRAKIS K., KUMMERER N., FOGlierini M., SERRANO L.: 'Noise in transcription negative feedback loops: simulation and experimental analysis', *Mol. Syst. Biol.*, 2006, **2**, (41)
- [15] RAJ A., VAN OUDENAARDEN A.: 'Single-molecule approaches to stochastic gene expression', *Annu. Rev. Biophys.*, 2009, **38**, pp. 255–270
- [16] SHAPIRO H.: 'Practical flow cytometry' (Wiley-Liss, 2003, 4th edn.)
- [17] RAJ A., VAN DEN BOGAARD P., RIFKIN S., VAN OUDENAARDEN A., TYAGI S.: 'Imaging individual mRNA molecules using multiple singly labeled probes', *Nat. Methods*, 2008, **5**, pp. 877–887
- [18] GILLESPIE D.T.: 'Exact stochastic simulation of coupled chemical reactions', *J. Phys. Chem.*, 1977, **81**, pp. 2340–2360

- [19] GILLESPIE D.T.: 'The chemical langevin equation', *J. Chem. Phys.*, 2000, **113**, pp. 297–306
- [20] ALLEN R., WARREN P., REIN TEN WOLDE P.: 'Sampling rare switching events in biochemical networks', *Phys. Rev. Lett.*, 2005, **94**, paper no. 018104
- [21] WARMFLASH A., BHIMALAPURAM P., DINNER A.: 'Umbrella sampling for nonequilibrium processes', *J. Chem. Phys.*, 2007, **127**, article id 154112
- [22] GILLESPIE D.T.: 'Approximate accelerated stochastic simulation of chemically reacting systems', *J. Chem. Phys.*, 2001, **115**, pp. 1716–1733
- [23] RAO C.V., ARKIN A.P.: 'Stochastic chemical kinetics and the quasi-steady-state assumption: application to the gillespie algorithm', *J. Chem. Phys.*, 2003, **118**, pp. 4999–5010
- [24] CAO Y., GILLESPIE D., PETZOLD L.: 'The slow-scale stochastic simulation algorithm', *J. Chem. Phys.*, 2005, **122**, paper no. 014116
- [25] VAN KAMPEN N.: 'Stochastic processes in physics and chemistry' (Elsevier, 2007, 3rd edn.)
- [26] ELF J., EHRENBERG M.: 'Fast evaluations of fluctuations in biochemical networks with the linear noise approximation', *Genome Res.*, 2003, **13**, pp. 2475–2484
- [27] NASELLI.: 'An extension of the moment closure method', *Theor. Popul. Biol.*, 2003, **64**, pp. 233–239
- [28] GMEZ-URIBE C., VERGHESE G.: 'Mass fluctuation kinetics: capturing stochastic effects in systems of chemical reactions through coupled mean–variance computations', *J. Chem. Phys.*, 2007, **126**, paper no. 024109
- [29] SINGH A., HESPANHA J.: 'A derivative matching approach to moment closure for the stochastic logistic model', *Bull. Math. Biol.*, 2007, **69**, pp. 1909–1925
- [30] SINITSYN N., HENGARTNER N., NEMENMAN I.: 'Adiabatic coarse-graining and simulations of stochastic biochemical networks', *Proc. Natl. Acad. Sci. USA.*, 2009, **106**, (26), pp. 10546–10551
- [31] WALCZAK A., MUGLER A., WIGGINS C.: 'A stochastic spectral analysis of transcriptional regulatory cascades', *Proc. Natl. Acad. Sci.*, 2009, **106**, (16), pp. 6529–6534
- [32] MUNSKY B., KHAMMASH M.: 'The finite state projection algorithm for the solution of the chemical master equation', *J. Chem. Phys.*, 2006, **124**, article id 044104
- [33] BURRAGE K., HEGLAND M., MACNAMARA S., SIDJE R.: 'A Krylov-based finite state projection algorithm for solving the chemical master equation arising in the discrete modelling of biological systems'. Proc. A.A.Markov 150th Anniversary Meeting, 2006, pp. 21–37
- [34] MUNSKY B., KHAMMASH M.: 'The finite state projection approach for the analysis of stochastic noise in gene networks', *IEEE Trans. Autom. Contr./IEEE Trans. Circuits Syst.*, 1, 2008, **52**, pp. 201–214
- [35] MUNSKY B.: 'The finite state projection approach for the solution of the chemical master equation and its application to stochastic gene regulatory networks'. PhD thesis, University of California at Santa Barbara, Santa Barbara, 2008
- [36] CAGATAY T., TURCOTTE M., ELOWITZ M., GARCIA-OJALVO J., SUEL G.: 'Architecture-dependent noise discriminates functionally analogous differentiation circuits', *Cell*, 2009, **139**, (3), pp. 512–522
- [37] WARMFLASH A., DINNER A.: 'Signatures of combinatorial regulation in intrinsic biological noise', *Proc. Natl. Acad. Sci. USA*, 2008, **105**, (45), pp. 17262–17267
- [38] DUNLOP M., COX III R., LEVINE J., MURRAY R., ELOWITZ M.: 'Regulatory activity revealed by dynamic correlations in gene expression noise', *Nat. Genet.*, 2008, **40**, pp. 1493–1498
- [39] DE RONDE W., DANIELS B., MUGLER A., SINITSYN N., NEMENMAN I.: 'Mesoscopic statistical properties of multistep enzyme-mediated reactions', *IET Syst. Biol.*, 2009, **3**, (5), pp. 429–437
- [40] MUNSKY B., TRINH B., KHAMMASH M.: 'Listening to the noise: random fluctuations reveal gene network parameters', *Mol. Syst. Biol.*, 2009, **5**, (318)
- [41] THORSLEY D., KLAVINS E.: 'Approximating stochastic biochemical processes with wasserstein pseudometrics', *IET Syst. Biol.*, 2010, **4**, (3), pp. 193–211
- [42] GARDNER T., CANTOR C., COLLINS J.: 'Construction of a genetic toggle switch in escherichia coli', *Nature*, 2000, **403**, pp. 339–342
- [43] KOBAYASHI H., KAERN M., ARAKI M., ET AL.: 'Programmable cells: interfacing natural and engineered gene networks', *Proc. Natl. Acad. Sci.*, 2004, **101**, pp. 8414–8419
- [44] WARREN P., REIN TEN WOLDE P.: 'Chemical models of genetic toggle switches', *J. Phys. Chem. B*, 2005, **109**, pp. 6812–6823
- [45] LIPSHTAT A., LOINGER A., BALABAN N., BIHAM O.: 'Genetic toggle switch without cooperative binding', *Phys. Rev. Lett.*, 2006, **96**, article id 188101
- [46] MUNSKY B., KHAMMASH M.: 'A multiple time interval finite state projection algorithm for the solution to the chemical master equation', *J. Comput. Phys.*, 2007, **226**, (1), pp. 818–835